We are IntechOpen, the world's leading publisher of Open Access books Built by scientists, for scientists

4,800
Open access books available

122,000
International authors and editors

135M
Downloads

Our authors are among the

154
Countries delivered to

TOP 1%
most cited scientists

12.2%
Contributors from top 500 universities

CLARIVATE ANALYTICS BOOK CITATION INDEX INDEXED

WEB OF SCIENCE™

Selection of our books indexed in the Book Citation Index in Web of Science™ Core Collection (BKCI)

Interested in publishing with us?
Contact book.department@intechopen.com

Numbers displayed above are based on latest data collected.
For more information visit www.intechopen.com

18

Flow Properties and Heat Transfer of Drag-Reducing Surfactant Solutions

Takashi Saeki
Yamaguchi University
Japan

1. Introduction

The frictional resistance of fluids can be reduced by adding small amounts of certain polymers, a phenomenon first reported (Toms, 1948) known as drag reduction or Toms phenomenon. The added polymers might form thread-like structures in fluids, which interact with turbulent eddies due to their viscoelasticity. Since the polymer synthesis technology and cost effectiveness have been highly improved, polymer drag reduction has been adopted widely in large pipeline systems for crude oils and refined petroleum products. Presently, more than 40% of all the gasoline consumed in the United States has polymer drag reducer in it (Motier, 2002). However, mechanical degradation of polymer chains in high shear rate regions, such as pumps, is frequently observed, which lowers the molecular weight and causes a loss of drag reduction. For that reason, polymer drag reduction cannot be adopted for circulating flow systems.

Drag reduction caused by surfactant solutions was first reported by Gadd (Gadd, 1966). Combinations of certain cationic surfactants with a suitable counter ion are often chosen as the drag-reducing agents. Some nonionic surfactants also show the drag-reducing effects, rendering the use of counter ions dispensable. A number of authors have pointed out that the surfactant molecules come together to form rod-like micelles, which are necessary for drag reduction. Figure 1 shows surfactant molecule and micelle structures. Drag-reducing surfactants form rod-like micelles, and their aggregates might be present in a solution. Figure 2 shows a transmission electron microscope (TEM) image of surfactant micelles (Shikata et al., 1988). Again, aggregates of rod-like micelles might interact with turbulent eddies and cause drag reduction. These aggregates suffer mechanical degradation in high shear rate regions, which is then repaired in lower shear stress regions, such as in flow through pipes.

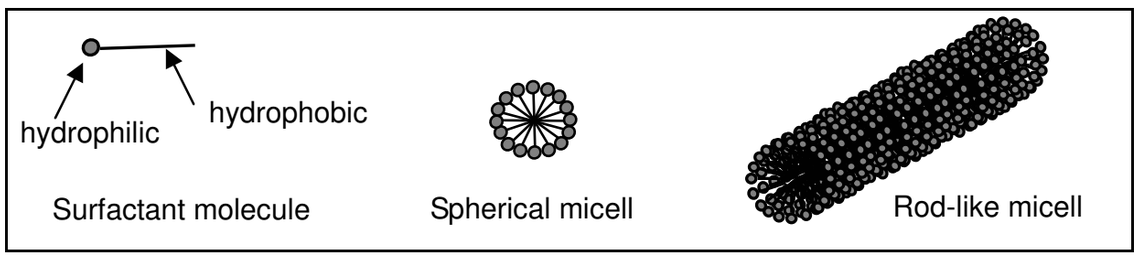

Fig. 1. Surfactant molecule and micelle structures

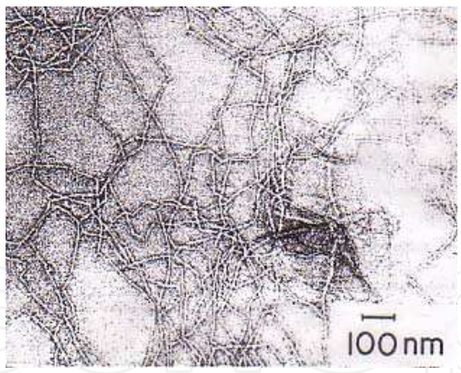

Fig. 2. Rod-like structure of surfactant micelles. (CTAB/NaSal. C_D=0.001 mol/L)

The drag reduction caused by surfactant solutions is considered to be an effective way to reduce the pumping power in closed-loop district heating and cooling systems. In 1994, a commercial application of surfactant drag reduction was first conducted in Japan by our group for the air conditioning system in the Shunan Regional Industry Promotion Center building (a two-story building with a total floor space of 2490 m²). We also developed commercially available drag-reducing additives (LSP-01A/M, LSP Corporative Union) based on the mixture of a cationic surfactant and corrosion inhibitors. Since 1995, LSP-01 has been used practically at more than 150 sites in building air conditioning systems throughout Japan, including office buildings, hotels, hospitals, supermarkets, airport facilities, and industrial factories. Quantitative evaluations of the energy conservation rate were conducted for each application project. Almost all of our drag-reducing projects showed more than a 20% reduction in the pumping power required for circulating water; furthermore, some air conditioning systems have obtained up to 50% energy savings with LSP-01 (Saeki et al., 2002). Table 1 shows some examples of our projects.
In the following section, several drag-reducing surfactants and their flow properties are summarized. Some studies have shown that heat transfer reduction occurs simultaneously for drag-reducing flows. Therefore in the next section, heat transfer characteristics obtained for our laboratory experiments are displayed for two commercially available drag-reducing surfactants, that are used frequently in practical facilities. In the last section, drag reduction and heat transfer data measured for our university library building are presented and evaluated with regard to the heat transfer characteristics of a practical air conditioning system before and after introducing surfactant drag reduction. We believe this information will be useful for future designs incorporating this technology.

2. Several drag-reducing surfactants and their flow properties

Many studies of surfactant drag reduction have been conducted since the 1980s, including investigations of the selection and optimization of additives, the drag reduction flow properties, the mechanism of drag reduction, and so on. Cetyl-trimethyl-ammonium chloride (CTAC, $C_{16}H_{33}N^+$ $(CH_3)_3Cl^-$) with sodium salicylate (HOC_6H_4COONa, called NaSal) displays significant drag reduction qualities, and many researchers have used these additives. However, it was found that the solution lost its solubility in water at temperatures lower than 7 °C, and some ions dissolved in tap water affected the drag reduction caused by CTAC. Therefore, screening tests of surfactants had been conducted (Ohlendorf et al., 1986; Chou et al., 1989; Usui et al., 1998). At the present, oreyl-bishydroxyethyl-methyl-ammonium

chloride ($C_{18}H_{35}N^+(C_2H_4OH)_2CH_3Cl^-$ brand name Ethoquad O/12) and oreyl-trishydroxyethylethyl-ammonium chloride ($C_{18}H_{35}N^+(C_2H_4OH)_3Cl^-$ brand name Ethoquad O/13) are used as suitable drag-reducing surfactants in Japan. Both surfactants have to be used in combination with a counter ion, NaSal. Stearyl-trimethyl-ammonium chloride (STAC, $C_{18}H_{33}N^+(CH_3)_3Cl^-$) was also selected as a drag-reducing surfactant for higher-temperature use, and a surfactant having an alkyl group carbon number of 22 shows effective drag reduction even over 100 °C (Chou et al., 1989). The molecular weights of these surfactants are several hundreds.

No.	Facility	Heat origin	Pump	Operating time (hours/year)	Water capacity (m^3)	Energy saving rate (%)
1	Home for the aged	ACWGM(90RT) ×1	5.5kW×1, 1.5kW×2	8,760	3	39
2	Factory 1	ACWGM(360RT) ×2 Turbo(400RT) ×1	45kW×3	4,380	25	21
3	Factory 2	ACWGM(160RT) ×2	22kW×2	2,100	10	27
4	Department store 1	ACWGM(450RT) ×2 Turbo(400RT) ×1	22kW×3	3,850	30	33
5	Department store 2	ACWGM(400RT) ×1 Turbo(315RT) ×1	37kW×1	4,420	7	29
6	Department store 3	ACWGM(600RT) ×1, (150RT) ×1	55kW×1, 22kW×2, 18.5kW×2	2,640	15	54
7	Hotel 1	ACWGM(300RT) ×3	22kW×2, 18.5kW×2, 11kW×2, 7.5kW×2	8,760	50	41
8	Hotel 2	ACWGM(125RT) ×1	15kW×1	8,000	10	48
9	Hotel 3	ACWGM(100RT) ×3	11kW×1, 7.5kW×1	2,000	15	48

ACWGM: Absorption Cooling Water Generating Machine Turbo: Turbo refrigerator

Table 1. Drag-reducing project with LSP-01

Figure 3 presents the friction factor versus Reynolds number data for water with different concentrations of LSP-01. LSP-01 contains 10% Ethoquad O/12, so in the case of 5000 mg/L LSP-01, for example, the solution contains 500 mg/L Ethoquad O/12, 300 mg/L NaSal, and corrosion inhibitors. Since drag-reducing solutions are non-Newtonian fluids, the viscosity used for the calculation of Reynolds number is used as the property of water. The drag

reduction increased with the Reynolds number and reached the maximum point (maximum drag reduction at a certain temperature). The maximum drag reduction percent ($DR\%$) is almost 70% for 5000 mg/L LSP-01. When the Reynolds number was further increased, the drag reduction was lost rather abruptly. This phenomenon may be caused by the breakup of the surfactant micelle structures due to high shear.

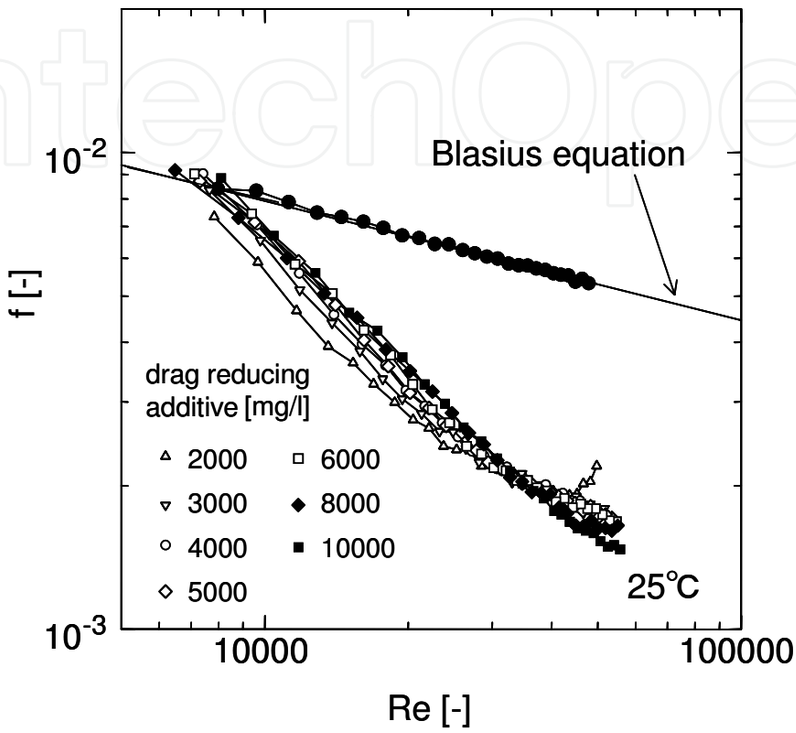

Fig. 3. Drag reduction results for LSP-01 at different temperatures

Figure 4 shows photos of water and a drag-reducing solution stirred in a beaker. Water shows a big eddy, while the drag-reducing solution shows no eddies due to the Weissenberg effect.

Water LSP-01(5000mg/L)

Fig. 4. Photos of water and a drag-reducing solution stirred in a beaker

Saeki et al. (2000) measured the flow characteristics of a drag-reducing surfactant by using particle tracer velocimetry (PTV) to study the mechanism of drag reduction. In the experimental results, the intensity of the fluctuation in the axial direction was high, while that in the radial direction was low but not zero. Despite the fluctuations occurring in the drag-reducing surfactant solution flow, the Reynolds stress was shown to be zero. Hence the drag-reducing flow is considered to be neither "turbulent" nor "laminar" and is assumed to be a kind of "transitional flow."

3. Heat transfer characteristics of drag-reducing flow

3.1 Review of related works

Not a few researchers have pointed out that heat transfer reduction occurs simultaneously for drag-reducing flows. Usui and Saeki (1993) measured the heat transfer characteristic of CTAC solution and reported that the analogy between momentum and heat transfer was invalid for drag reduction flow and that the heat transfer reduction was as high as to be even larger than the drag reduction rate. Aguilar et al. (2001) introduced both a maximum heat transfer reduction asymptote (MHTRA) and a maximum drag reduction asymptote (MDRA) for surfactant solutions. They indicated that the ratio of MHTRA and MDRA could be expressed with a constant value of 1.06, independent of the Reynolds number. Steiff et al. (1998) noted that the influence of drag-reducing additives on heat exchangers had to be given particular attention and recommended several ways to improve the heat output behavior of heat exchangers. Qi et al. (2001) reported the enhanced heat transfer of drag-reducing surfactant solutions with a fluted tube-in-tube heat exchanger. In their experiments, there was a surprising increase in the heat transfer reduction with Ethoquad T13-50 solution at a temperature of 60 °C, even though the pressure drop in the solution at this temperature is close to that of water in the fluted tube. They pointed out that this temperature is near the upper temperature limit for drag reduction of the solution and noted the possibility that the heat transfer reduction decreases slowly with the Reynolds number.

In a normal air conditioning system, the temperature of circulating water is around 60 °C, and LSP-01 shows a sufficient and stable drag-reducing rate at this temperature range. However, it is expected that the temperature inside a heat exchanger will be higher, and it should coincide with the upper limit temperature of drag reduction with LSP-01. In this study, two drag-reducing additives were used, and both drag reduction and heat transfer reduction were measured from room temperature to that beyond the upper limit temperatures of drag-reducing solutions.

3.2 Experimental procedure and data reduction

The cationic surfactants used were Ethoquad O/12 (oreyl-bishydroxyethyl-methyl - ammonium chloride) and Ethoquad O/13 (oreyl-trishydroxyethylethyl-ammonium chloride) produced by Lion Akzo Corporation, Japan. The counter ion selected was sodium salicylate (NaSal). In the case of Ethoquad O/12, the 1.23 mM (500 mg/l) surfactant was mixed with 2.08 mM (300 mg/l) NaSal and water, a mixing rate that shows good drag reduction. Since a similar mixing rate is suitable for Ethoquad O/13, the experiments were conducted with the weight ratio of both surfactants and NaSal kept at 1.67. The experimental apparatus used for drag reduction and heat transfer experiments was a recirculation system, as shown in Figure 5. Drag-reducing agents were added to a tank, and

solutions were prepared. The temperature of the solutions was controlled by using a heater with a temperature control device to allow experiments to run from room temperature to 80 °C. The flow rate was controlled by an inverter system installed on then system's main pump.

The pressure drop test section was a straight PVC pipe, 1600 mm long, 14.5 mm inside diameter. Measurements were carried out using an electric differential manometer. The heat transfer test section consisted of a copper tube, an electric heater, and heat insulators. The copper tube was a practical heat exchanger tube, 1500 mm long, 14.5 mm inside diameter, 17.1 mm outside diameter. A cross-sectional view of the test section of the heat transfer experiment is shown in Figure 5. An electric heater of constantan wire insulated with glass fiber and calcium silicate insulator was used to obtain a constant heat flux condition during the test section. The heated surface temperature was measured at a point 1500 mm from the inlet by a K-type thermocouple buried in the copper pipe (depth =0.5 mm). The inlet and outlet temperatures of the test section were also measured. The outlet temperature was measured at a mixing box installed just after the test section. Three K-type thermocouples were fixed at different positions inside the mixing box, and the average temperature was calculated. All the data were obtained over 5 minutes and averaged. The difference temperature between the inlet and outlet of the heat transfer test section was set to more than 2 °C but less than 5 °C throughout the experiments.

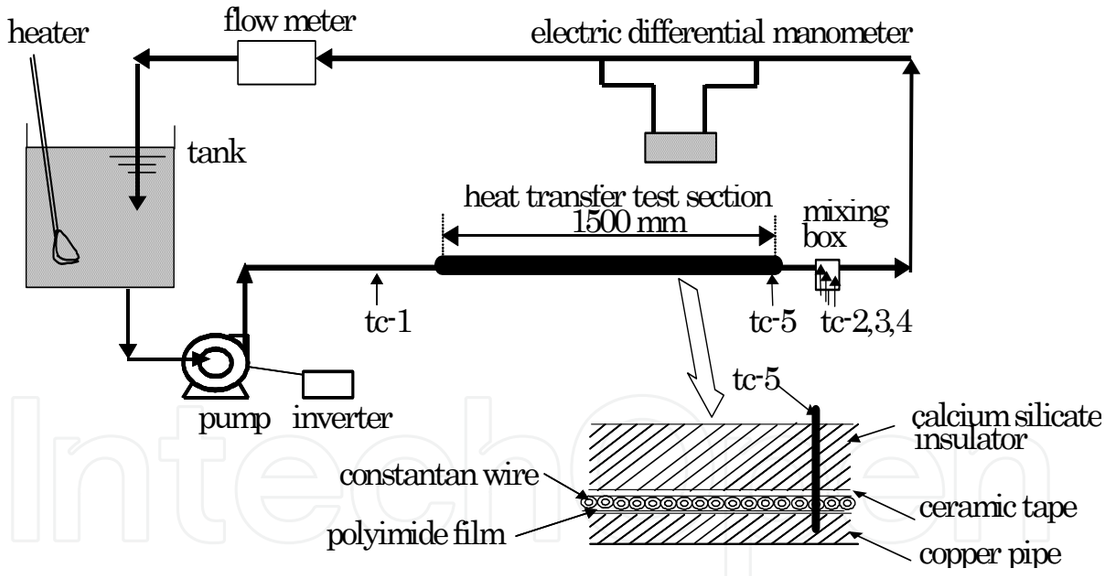

Fig. 5. Experimental apparatus

During drag reduction tests, the temperature of the test solution was kept constant throughout the test loop. The Reynolds number was calculated with the property of water. For convenient comparison of the drag reduction results between water and test solutions, the drag reduction rate, $DR\%$, was defined as follows:

$$DR\% = \frac{f_w - f_{DR}}{f_w} \times 100 \tag{1}$$

in which the friction factor of water, f_w , was obtained by using the Blasius equation (f_w =0.0791Re$^{-0.25}$), while that of surfactant solution, f_{DR} , was measured. For the heat transfer tests, both Reynolds and Prandtl numbers were calculated with the property of the solvent at the average temperature of the inlet and outlet of the test section. The amount of heat flow was calculated as follows:

$$Q = GC_p(T_{out} - T_{in}) \tag{2}$$

where G, C_p, T_{out}, and T_{in} are the flow rate, specific heat, outlet temperature, and inlet temperature of the test section, respectively. By using measured outer surface temperature, the inner surface temperature could be calculated as follows:

$$T_2 = T_1 - \frac{Q(r_1 - r_2)}{kA_{im}} \tag{3}$$

where r, k, and A_{lm} are the tube radius, thermal conductivity, and logarithmic mean of heat surface area, respectively. The subscripts of 1 shows outer surface, while 2 indicates inner surface. By assuming that the temperature through the test section increased linearly from the inlet to the outlet temperature, we were able to calculate a fluid temperature at the position where the thermocouple was buried and the difference between the temperature and T_2 was defined as ΔT. Then, the heat transfer coefficient, h, was calculated as follows:

$$h = \frac{Q}{\Delta T A_2} \tag{4}$$

Finally, the Nusselt number (= hD/k) was obtained. Here, for a convenient comparison of the heat transfer results between water and the test solutions, we defined the heat transfer reduction rate, $HTR\%$, as follows:

$$HTR\% = \frac{h_w - h_{DR}}{h_w} \times 100 \tag{5}$$

3.3 Results and discussion

Figure 6 shows the friction factors, f, and the Reynolds numbers, Re, for water and Ethoquad O/12 with NaSal solutions at different concentrations measured at 30 °C. All points for the water test lay close to the Blasius equation, with a deviation of less than 5%. For surfactant solutions, the drag reduction increased with the Reynolds number and reached a maximum point. When the Reynolds number was further increased, the drag reduction was lost rather abruptly. This phenomenon might be related to the breakup of the surfactant micelle structures due to high shear. With increasing surfactant concentration, the maximum drag reduction was shifted to a higher Reynolds number.

Figure 7 gives the corresponding heat transfer test results for the solutions. The figure presents the relation between the $Nu/Pr^{0.4}$ values and the Reynolds numbers. Again, all points for the water test lay close to the Bittus-Boelter empirical equation for a Newtonian fluid with a deviation of less than 5%. For surfactant solutions, the heat transfer reduction increased with the Reynolds number. The 100 mg/l Ethoquad O/12 solution showed the maximum value and reached the Newtonian line at the higher Reynolds number region;

however, the 300 mg/l and 500 mg/l solutions maintained a high level of heat transfer reduction. There was a significant decrease of drag reduction with an increase in the Reynolds number; however, the $Nu/Pr^{0.4}$ kept almost constant values with the 300mg/l and 500mg/l solutions. Qi et al. (2001) reported similar results with Ethoquad T13-50 solution.

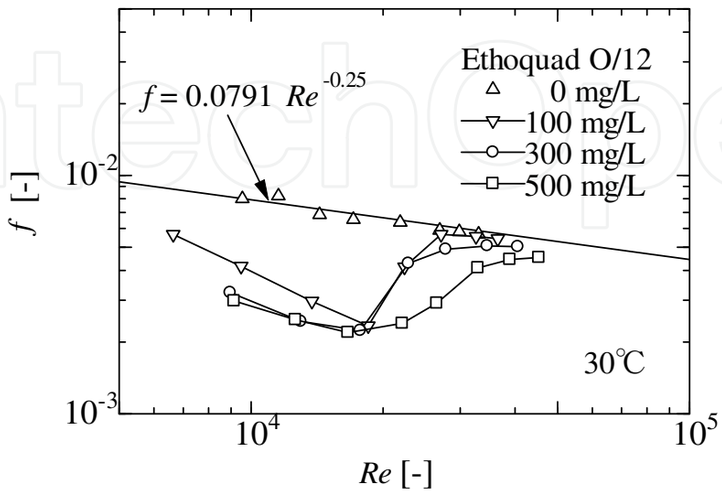

Fig. 6. Drag reduction results for Ethoquad O/12 and NaSal systems at different concentrations at 30 °C

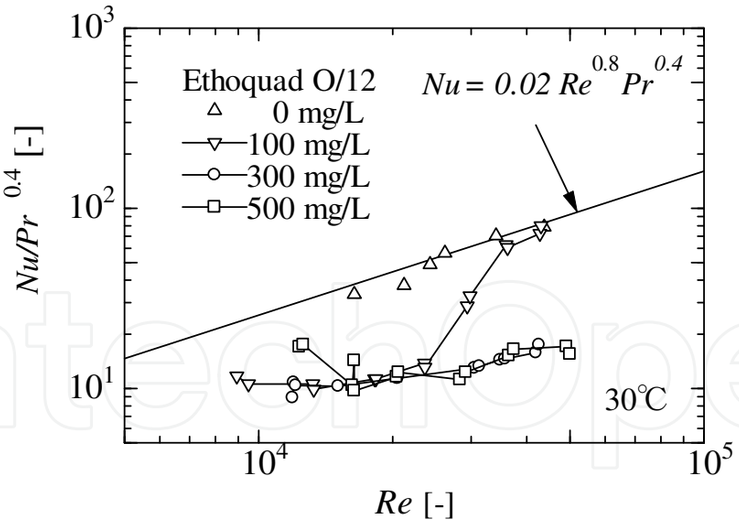

Fig. 7. Heat transfer results for Ethoquad O/12 and NaSal systems at different concentrations at 30 °C

Figure 8 shows *f* vs. *Re* for Ethoquad O/12 solutions at 50 °C. Drag reduction endured to a higher Reynolds number compared with the results at 30 °C. The 100 mg/L solution showed significant drag reduction compared with the 300 mg/L and 500 mg/L solutions; however, the drag reduction was lost rather abruptly when the Reynolds number exceeded 35,000.

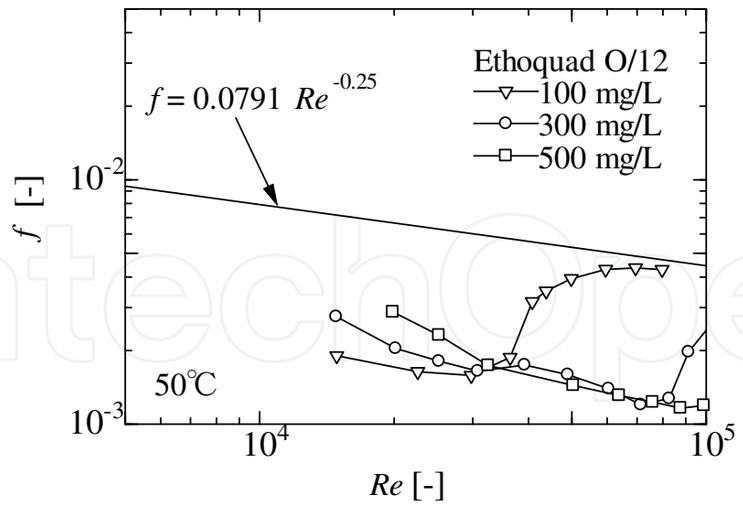

Fig. 8. Drag reduction results for Ethoquad O/12 and NaSal systems at different concentrations at 50 °C

Figure 9 shows the corresponding $Nu/Pr^{0.4}$ vs Re at 50 °C. The reduction rate of $Nu/Pr^{0.4}$ is lower than that for the 300 mg/L and 500 mg/L solutions. Experimental results of drag reduction and heat transfer characteristics varied with the concentration of Ethoquad O/12, Reynolds number (flow velocity), and temperature of the solutions. As these results show the analogy between momentum and heat transfer is invalid for drag-reducing flows.

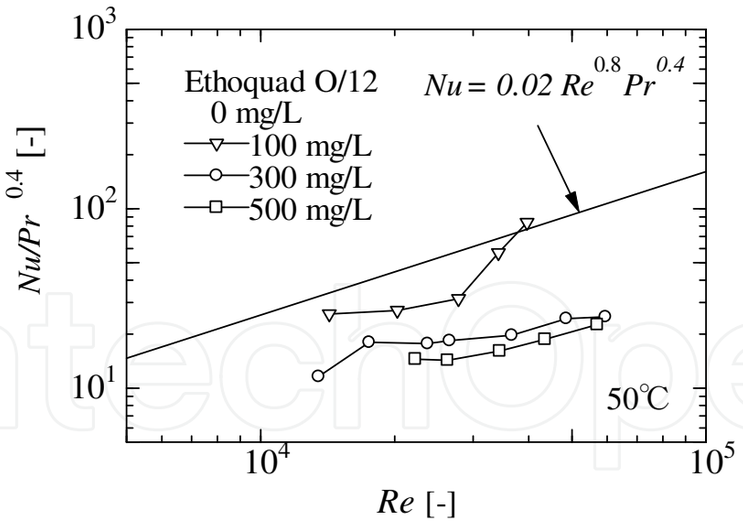

Fig. 9. Heat transfer results for Ethoquad O/12 and NaSal systems at different concentrations at 50 °C

Figure 10 shows the relationship between $DR\%$ and solution temperature. Experiments were conducted to increase the temperature of 500 mg/l Ethoquad O/12 solution gradually from room temperature to 75 °C. The velocity at the test sections was kept constant at 1.5 m/s, corresponding to the typical velocity inside a practical heat transfer pipe. It is clear that with increasing solution temperature, drag reduction increased and a maximum $DR\%$ of

75% was observed from 60 °C to 65 °C. Over this temperature range, drag reduction was suddenly lost. In this paper, the upper limit temperature is defined as the temperature that shows a 50 percent *DR%*, as shown in Fig. 10. Although the value, 50%, has no particularly important meaning, the criteria can be applied in that the micelle structure of the surfactant changes due to the heat of a solution.

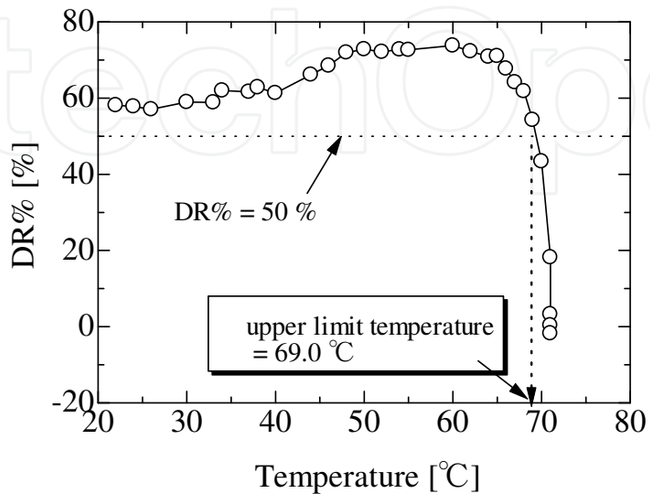

Fig. 10. Temperature dependence of drag reduction with 500 mg/l Ethoquad O/12 and 300 mg/l NaSal

Figure 11 shows *DR%* and *HTR%* of Ethoquad O/12 at different concentrations and temperature conditions. In the case of 100 mg/l solution, the upper limit temperature of drag reduction is 52 °C. We note that *HTR%* is less than *DR%* when the temperature is higher than the upper limit temperature. In the case of 300 mg/l solution, the upper limit temperature is 68 °C, and a similar relation between *DR%* and *HTR%* can be observed.

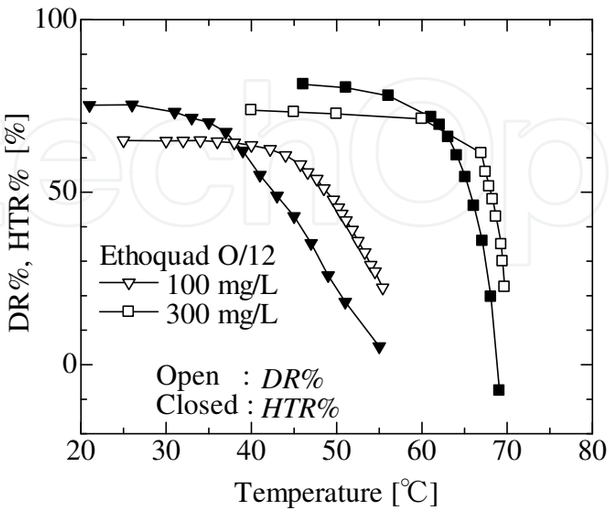

Fig. 11. *DR%* and *HTR%* of Ethoquad O/12 at different concentrations and temperatures. Average velocity of the flow was set at 1.2 m/s

Previous works on heat transfer enhancement have focused on the significant heat transfer reduction rather than drag reduction, but we want to stress that the suitable additive condition for an air conditioning system exist for Ethoquad O/12, which shows higher *DR%* with lower *HTR%*. It is also important to keep the concentration of a drag-reducing additive at a suitable value that can restrain the heat transfer reduction inside the heat exchanger and also provide enough drag reduction through the pipeline.
Figure 12 shows both the *DR%* and *HTR%* of Ethoquad O/13 in comparison with the results with Ethoquad O/12. The results show that twice as much Ethoquad O/13 as Ethoquad O/12 is needed to obtain the similar level of *DR%*.

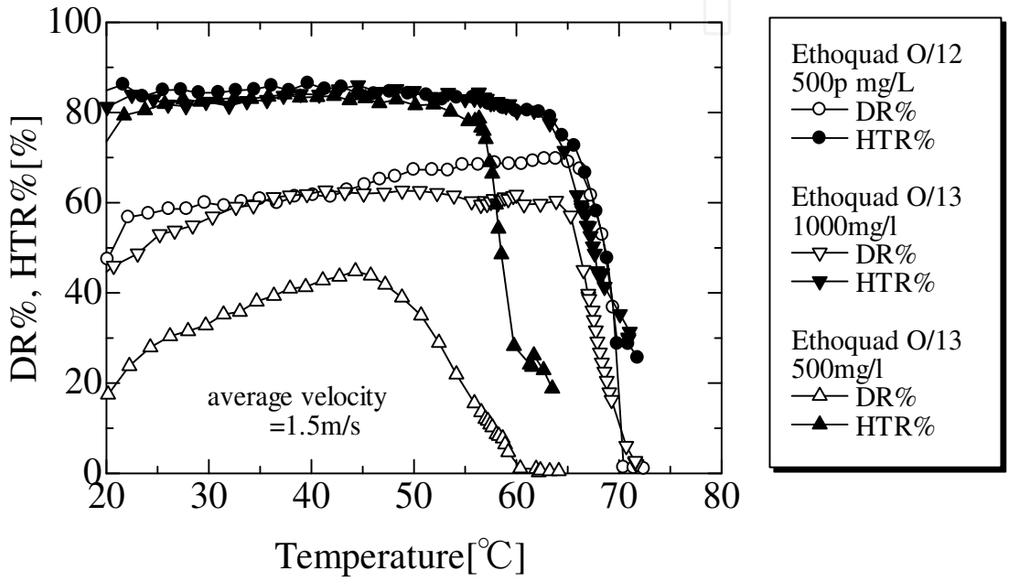

Fig. 12. *DR%* and *HTR%* of Ethoquad O/13 at different concentrations and temperatures. Average velocity of the flow was set at 1.5 m/s

Since the production cost of Ethoquad O/12 is cheaper, the drag-reducing additive produced with Ethoquad O/12 has better cost effectiveness. When the concentration of Ethoquad O/13 decreased due to water leakage from the system during long-term operation, it is likely that the drag reduction decreased significantly. The suitable additive condition for Ethoquad O/13, which shows higher *DR%* with lower *HTR%*, was not found in this study.

4. Evaluation of the heat transfer characteristics of a practical air conditioning system before and after introducing surfactant drag reduction

4.1 Objective

In the preceding section, heat transfer reduction was presented for drag reduction flows, especially in the case of unsuitable additive conditions. It is not easy to measure the heat transfer rate accurately for practical air conditioning systems in usual operation; however, according to our projects with LSP-01, no predicted serious problem of heat transfer has been detected. It is necessary to obtain quantitative heat transfer characteristics for a

practical air conditioning system. In this study, drag reduction and heat transfer data measured at our university library building is presented as an example of application in a practical air conditioning system.

4.2 Experimental procedure

The library building of Yamaguchi University (Figure 13) is two stories with the total floor space of 2,400 m^2. Each floor has its own pipeline system with a heat pump and a chiller unit (40 RT, 33 kW, Figure 14). Figure 15 shows a schematic diagram of the air conditioning system. Produced cold or hot water is transported to an air conditioner at the first floor in a machine room to exchange heat with the air. The temperatures of each position mentioned in the figure were measured continuously by using resistance bulb thermometers. The water flow rate was measured by an ultrasonic flow meter (Model UFP-20, Tohki Sangyo, Japan). All the data were stored in a PC and analyzed.

Fig. 13. Yamaguchi University library building

Fig. 14. Heat pump - chiller units

Experiments were conducted for almost one month during both the summer and winter seasons in 2007. In the summer season, operation conditions of the air conditioning system without drag-reducing additives were as follows:

1. The system was started at 7:30 every morning. At this time, the temperature of the circulating water was around 22 °C.
2. The chiller unit produced cold water. When the circulating water temperature became 11 °C, the unit stopped.
3. When the circulating water temperature became 18 °C, the chiller unit started automatically.

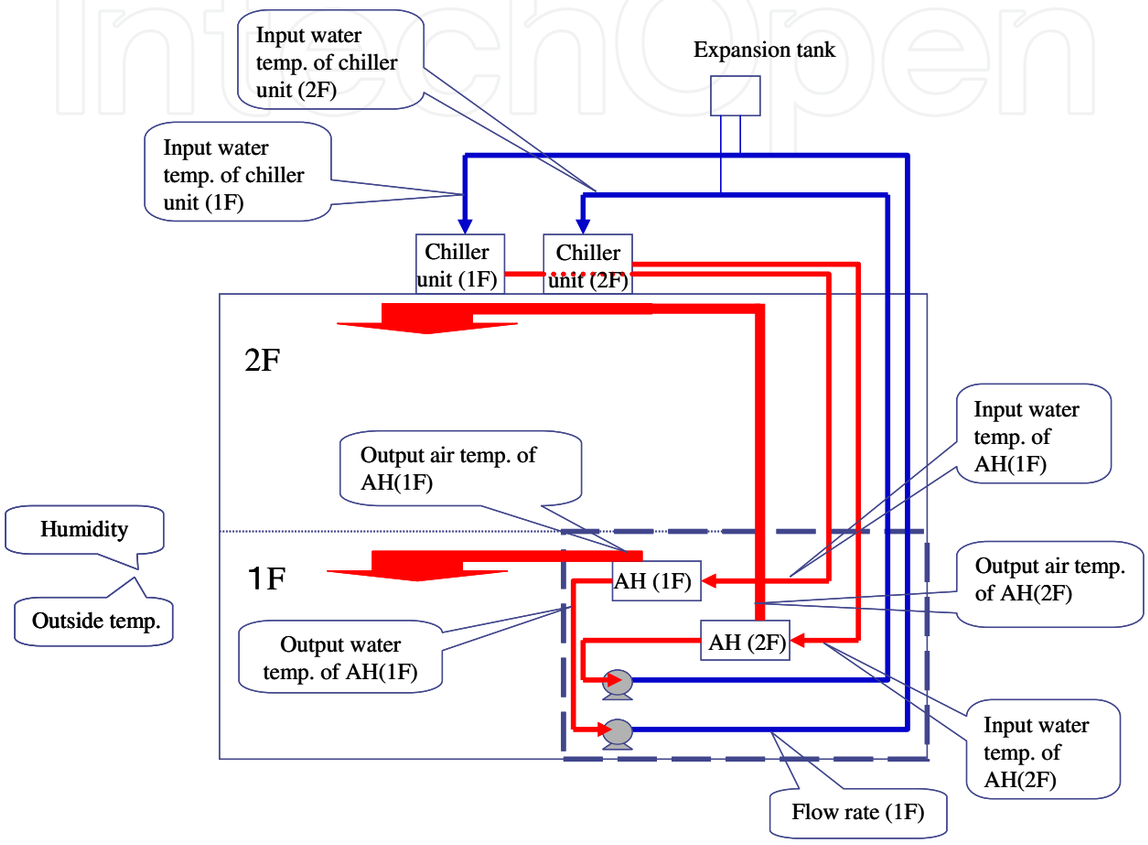

Fig. 15. Schematic diagram of the air conditioning system. (AH: Air Handling Unit)

After accumulating data for two weeks, we added LSP-01M, which included Ethoquad O/12, NaSal, and sodium molybdate as a corrosion inhibitor, to the system (Figure 16). The concentration of LSP-01M was 5000 mg/L, and thus the surfactant concentration was 500 mg/L.

4.3 Experimental results

The water flow rate increased from 5.7 L/s to 6.01 L/s with the addition of 5000 mg/L LSP-01. To adjust the flow rate to the former value (5.7 L/s) by controlling an inverter system installed on the main pump, we changed the electric current of the pump from 5.4 A to 4.5A, and as a consequence, 16.7% reduction of energy consumption was obtained. In the analyses of all the stored temperature data for a month, we found no significant difference between before and after the addition of the drag-reducing additive. The operation of this air conditioning system can be summarized as follows:

1. Measure the output water temperature of the chiller unit.
2. If the measured temperature is higher than an upper setting temperature, run the chiller unit.
3. If the measured temperature is lower than a lower setting temperature, stop the chiller unit.

Fig. 16. Addition of LSP-01 from the discharged side of the main pump

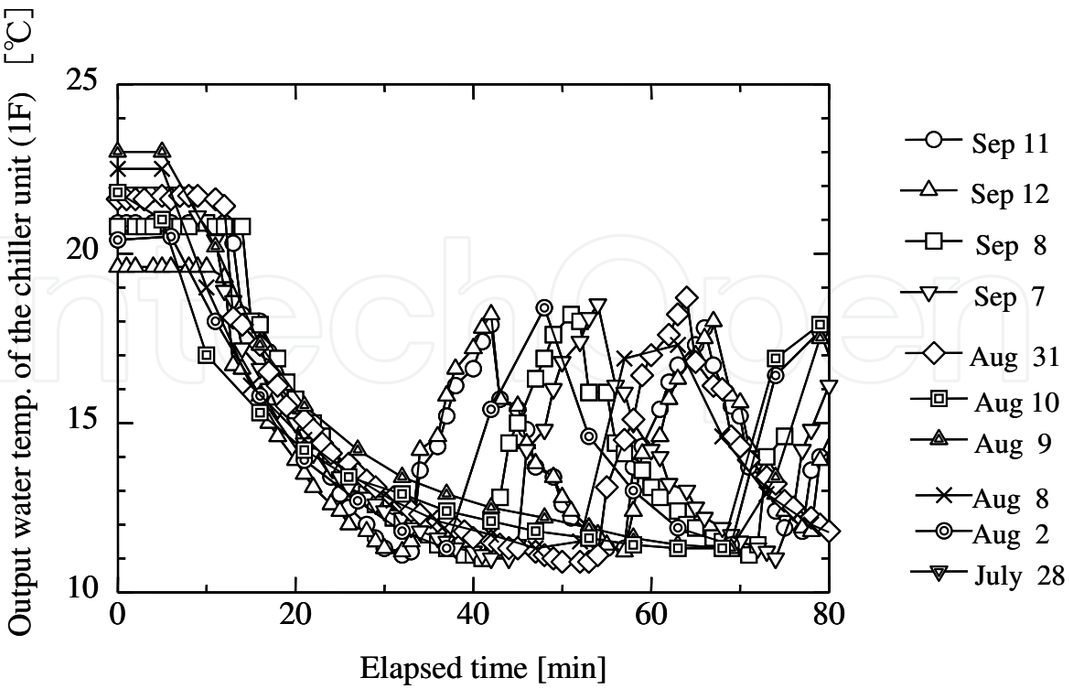

Fig. 17. Output water temperature versus elapsed time for of the chiller unit (1F)

If the heat transfer reduction caused by the drag-reducing additive occurs, the operating time of the chiller unit should be longer than the normal operation without the additive.
Figure 17 shows the output temperatures of the chiller unit (1F). The figure indicates that the temperatures were around 20 °C just before the operation of the air conditioning system. Then, the temperature decreased gradually after the chiller unit was run. After several tens of minutes, the chiller stopped and the temperature suddenly increased. If the temperature reached the upper setting temperature, the chiller started. Therefore, the temperature charts with respect to the elapsed times became zigzag shapes.
To determine the operating intervals of the chiller unit, the following function was used to fit the down side of the zigzag chart:

$$y = y_0 \exp\left(\frac{-t}{t_R}\right) \tag{6}$$

where y, y_0, t, and t_R are the output water temperature, constant, elapsed time, and relaxation time, respectively. The relaxation time can be used to evaluate the operating interval. Table 2 indicates the relaxation times for the down side of the first zigzag chart of each day. The drag-reducing additive was introduced on August 21st; however, the relaxation times did not show a significant change between before and after the addition.

Date	y_0	$1/t_R$	t_R [min]
July 28	20.0	0.0117	85.5
Aug 8	20.0	0.0155	64.5
Aug 9	19.6	0.0103	97.1
Aug 10	18.9	0.0093	107.5
Aug 31	18.0	0.0142	70.4
Sep 7	19.6	0.0189	52.9
Sep 8	18.1	0.0209	47.8
Sep 11	19.3	0.0317	31.5
Sep 12	17.4	0.0249	40.2

Table 2. Relaxation time for the down side of the first zigzag chart of each day

4.4 Discussion

In section 3, we described the measurement of the heat transfer characteristics for drag-reducing flow by the laboratory experimental apparatus, and a significant amount of heat transfer reduction was observed when the additive conditions were unsuitable. In section 4-3, we evaluated the possibility of a heat transfer reduction occurring and found no evidence of a heat transfer reduction. One of the following may have caused the difference in these results:
1) In the case of the laboratory experiment, the heat transfer characteristics were evaluated based on the reduction of the heat transfer coefficient between the wall of the copper pipe (heat exchanger) and water. Since it was impossible to measure the wall temperature of the

chilling unit, we used the temperature differences of the inlet and outlet of the chilling unit to evaluate the heat transfer characteristics. In other words, the heat transfer characteristics were evaluated based on the overall coefficient of heat transfer, U , which is determined the following equation:

$$\frac{1}{U} = \frac{1}{h_w} + \frac{x}{k} + \frac{1}{h_a} \tag{7}$$

where h_w, x, k, and h_a are the heat transfer coefficient of water, the thickness of the heat exchanger's wall, the thermal conductivity of the wall, and the heat transfer coefficient of air, respectively. Since h_w is two orders of magnitude larger than h_a, the value of U is not significantly changed even if the value of h_w is reduced due to the heat transfer reduction. To took at a quantitative example, let us assume the following values:

h_w=5800 W/m²·K for water flow

h_w=1200 W/m²·K for drag-reducing flow ($HTR\%$=80 %)

x=1 mm, k=350 W/mK, h_a=60 W/m²·K

The calculated overall heat transfer coefficient for water flow is 59.4 W/m²·K, while that for drag-reducing flow is 57.1 W/m²·K. As a result, the heat transfer reduction with respect to the overall heat transfer coefficient is only a 3.9% reduction, even though the heat transfer coefficient of fluid was reduced significantly.

2) In the case of the laboratory experiment, the constant heat flux conditions were maintained during the experiment, which means the difference of the inlet and outlet temperatures of the copper pipe did not affect the flow conditions. In this experiment, when the heat transfer occurred, the wall temperature increased. On the other hand, for the practical air conditioning system, the heat transfer phenomenon occurred unsteadily due to the intermittent operation of the chilling unit and inadequate mixing of the fluid. Therefore, even though the heat transfer reduction occurred in response to the drag-reducing additives, it was not easy to monitor the influence of the reduction of heat transfer.

3) Finally, we want to stress that micelle aggregates of drag-reducing surfactants normally suffer mechanical degradation in the chiller unit pipe of practical air conditioning systems. The average velocity inside heat exchangers is usually designed to be in the range of 1.5 m/s to 2.0 m/s. Also, practical pipelines have many elbows, branches, reduction or expansion pipes, valves, and so on, in which the shear rates applied to the fluids are larger than the rated in straight pipes. However, it is quite difficult to evaluate the drag reduction and the heat transfer reduction in the practical heat exchangers while factoring in the associated changes in the micelle structure of drag-reducing surfactants.

5. Conclusion

The drag-reducing technology will be applied to an ever increasing range of applications. There is also enormous potential for application of this approach to other fluids besides water, so we can expect a lot of research in this area. Finally, we observed certain characteristic near-wall momentum and heat transfer behavior in flows that calls for further investigation. This behavior is attributed to the effects of uneven transfer phenomena of micelle motion in pipes for drag-reducing flows, and investigation of this phenomenon should lead to new insights regarding the mechanism involved in drag-reducing flows.

6. Acknowledgment

The author would like to express his thanks to Mr. T. Matsumura, LSP Cooperative Union, and Mr. K. Tokuhara, Shunan Region Local Industry Promotion Center Foundation, for their valuable discussion on the drag reduction by surfactant solutions. The author also would like to acknowledge the experimental assistance of a student colleague (Yusuke Uchiyama).

7. References

Aguilar, G.; Gasljevic, K. & Matthys, E. J. (2001). Asymptotes of Maximum Friction and Heat Transfer Reductions for Drag-reducing surfactant Solutions, *Int. J. of Heat and Mass Transfer*, Vol.44, pp.2835-2843

Gadd, G. E. (1966). Reduction of Turbulent Friction in Liquids by Dissolved Additives, *Nature*, Vol. 212, pp. 874-877

Ohlendorf, D.; Interthal, W. & Hoffmann, H. (1986). Surfactant systems for drag reduction:physico-chemical properties and rheological behaviour, *Rheology Acta*, Vol. 25, pp.468-486

Qi, Y.; Kawaguchi, Y.; Lin, Z.; Ewing, M.; Christensen, R. & Zakin, J. (2001). Enhanced Heat Transfer of Drag Reducing Surfactant Solutions with Fluted Tube-in-tube Heat Exchanger, *Int. J. of Heat and Mass Transfer*, Vol.44, pp.1495-1505

Saeki, T.; De Guzman, M.; Morishima, H.; Usui, H. & Nishimura, T. (2000). A Flow Visualization Study on the Mechanism of Turbulent Drag Reduction by Surfactants, *Nihon Reoroji Gakkaishi*, Vol. 28, No.1, pp.35-40

Saeki, T.; Tokuhara, K.; Matsumura, T. & Yamamoto, S. (2002). Application of Surfactant Drag Reduction for Practical Air Conditioning Systems, *Nihon Kikai Gakkai Ronbunshu*, B, Vol. 68, No. 669, pp.1482-1488 (in Japanese)

Shikata T. et al. (1988). Micelle formation of detergent molecules in aqueous media. II: Role of free salicylate ions on viscoelastic properties of aqueous cetyltrimethylammonium bromide-sodium salicylate solutions, *Langmuir*, Vol. 4, pp. 354-359, 1988

Usui, H. & Saeki T. (1993). Drag Reduction and Heat Transfer Reduction by Cationic Surfactants, *J. of Chem. Eng. Japan*, Vol.26, No.1, pp.103-106

Usui, H. et al. (1998). Effect of surfactant molecular structure on turbulent drag reduction, *Kagaku Kogaku Ronbunshu*, Vol. 24, No.1, pp.134-137 (in Japanese)

Chou, L.-C.; Christensen, R. N. & Zakin, J. L. (1989). The influence of chemical composition of quaternary ammonium salt cationic surfactants on their drag reducing effectiveness, *Proceedings of 4th Int. Conf. on Drag Reduction*, Davos, IAHR/AIRH, Ellis Horwood Pub., pp.141-148

Motier, J. F. (2002). Polymer advances and the dramatic growth in commercial pipeline drag reduction, *Proceedings of 12th European Drag Reduction Meeting*, Herning, Denmark, April 18-20, 2002

Steiff, A.; Klopper, K. & Weinspach, P. (1998). Influence of Drag Reducing Additives in Heat Exchangers, *Proceedings of 11th IHTC*, 6, pp.317-322, Kyongju, Korea

Toms, B. A. (1948). Some observations on the flow of linear polymers solutions through straight pipe at large Reynolds numbers. *Proceedings of International Congress on Rheology*, Vol. 2, pp. 135-141, Scheveningen, Italy, 1948

Li, B.; Xu, Y. & Choi, J. (1996). Applying Machine Learning Techniques, *Proceedings of ASME 2010 4th International Conference on Energy Sustainability*, pp. 14-17, ISBN 842-6508-23-3, Phoenix, Arizona, USA, May 17-22, 2010

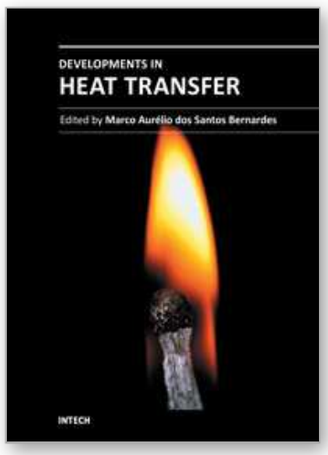

Developments in Heat Transfer

Edited by Dr. Marco Aurelio Dos Santos Bernardes

ISBN 978-953-307-569-3
Hard cover, 688 pages
Publisher InTech
Published online 15, September, 2011
Published in print edition September, 2011

This book comprises heat transfer fundamental concepts and modes (specifically conduction, convection and radiation), bioheat, entransy theory development, micro heat transfer, high temperature applications, turbulent shear flows, mass transfer, heat pipes, design optimization, medical therapies, fiber-optics, heat transfer in surfactant solutions, landmine detection, heat exchangers, radiant floor, packed bed thermal storage systems, inverse space marching method, heat transfer in short slot ducts, freezing an drying mechanisms, variable property effects in heat transfer, heat transfer in electronics and process industries, fission-track thermochronology, combustion, heat transfer in liquid metal flows, human comfort in underground mining, heat transfer on electrical discharge machining and mixing convection. The experimental and theoretical investigations, assessment and enhancement techniques illustrated here aspire to be useful for many researchers, scientists, engineers and graduate students.

InTech Europe
University Campus STeP Ri
Slavka Krautzeka 83/A
51000 Rijeka, Croatia
Phone: +385 (51) 770 447
Fax: +385 (51) 686 166
www.intechopen.com

InTech China
Unit 405, Office Block, Hotel Equatorial Shanghai
No.65, Yan An Road (West), Shanghai, 200040, China
中国上海市延安西路65号上海国际贵都大饭店办公楼405单元
Phone: +86-21-62489820
Fax: +86-21-62489821

IntechOpen